

A characteristic observable signature of preferred frame effects in relativistic binary pulsars

N. Wex, M. Kramer^{*}

University of Manchester, Jodrell Bank Observatory, Macclesfield, Cheshire, SK11 9DL, UK

ABSTRACT

In this paper we develop a consistent, phenomenological methodology to measure preferred-frame effects (PFEs) in binary pulsars that exhibit a high rate of periastron advance. We show that in these systems the existence of a preferred frame for gravity leads to an observable characteristic ‘signature’ in the timing data, which uniquely identifies this effect. We expand the standard Damour-Deruelle timing formula to incorporate this ‘signature’ and show how this new PFE timing model can be used to either measure or constrain the parameters related to a violation of the local Lorentz invariance of gravity in the strong internal fields of neutron stars. In particular, we demonstrate that in the presence of PFEs we expect a set of the new timing parameters to have a unique relationship that can be measured and tested incontrovertibly. This new methodology is applied to the Double Pulsar, which turns out to be the ideal test system for this kind of experiments. The currently available dataset allows us only to study the impact of PFEs on the orbital precession rate, $\dot{\omega}$, providing limits that are, at the moment, clearly less stringent than existing limits on PFE strong-field parameters. However, simulations show that the constraints improve fast in the coming years, allowing us to study all new PFE timing parameters and to check for the unique relationship between them. Finally, we show how a combination of several suitable systems in a *PFE antenna array*, expected to be available for instance with the Square-Kilometre-Array (SKA), provides full sensitivity to possible violations of local Lorentz invariance in strong gravitational fields in all directions of the sky. This PFE antenna array may eventually allow us to determine the direction of a preferred frame should it exist.

Key words: gravitation, pulsars:general, pulsars:individual:PSR J0737–3039

1 INTRODUCTION

The theory of general relativity (GR) has so far passed all experimental tests with flying colours (Stairs 2003, Will 2006, Kramer et al. 2006). Nevertheless, GR may not be the final word in our understanding of gravity and indeed, alternative theories of gravity exist, predicting deviations from GR in various possible ways.

Some theories of gravity predict that the Universe’s global matter distribution selects a preferred rest frame for local gravitational physics. In such theories the outcome of gravitational experiments depends on the motion of the laboratory with respect to this preferred frame. In particular, theories in which gravity is partially mediated by a vector field or a second tensor field are known to exhibit such preferred-frame effects whose strength is determined by cosmological matching parameters.

In the post-Newtonian limit, such preferred-frame effects are described by two phenomenological parameters, the parameterised post-Newtonian (PPN) parameters α_1 and α_2 . In GR these two parameters are zero. Solar system experiments have already tightly constrained these two PPN parameters. For details see Will (1993, 2006) and references therein. On the other hand, limits obtained in the weak gravitational fields of the solar system cannot rule out effects that only become significant in strong gravitational fields. For the well-motivated scalar-tensor theories, this has been demonstrated in a series of papers by Damour and Esposito-Farèse (1992a, 1993, 1996a, 1996b).

In order to describe preferred-frame effects in binary pulsars, Damour and Esposito-Farèse (1992b) introduced a non-boost-invariant Lagrangian that includes two strong field parameters $\hat{\alpha}_1$ and $\hat{\alpha}_2$, capable of accounting for strong-field violations of a local Lorentz invariance of gravity. In the weak-field limit these two strong-field parameter are equal to α_1 and α_2 , respectively. Concentrating on the contribution by $\hat{\alpha}_1$, Damour and Esposito-Farèse show that $\hat{\alpha}_1$ has the ef-

^{*} Email: Michael.Kramer@manchester.ac.uk

fect of inducing secular variations in the orbital eccentricity and in the orientation of the pulsar orbit, i.e. the location of periastron and the orientation of the orbital plane. These variations depend on the magnitude and direction of the velocity with respect to the preferred frame. Their calculations for small-eccentricity orbits shows that the eccentricity oscillates in a specific way between a maximum and a minimum value, with the period of the relativistic precession of periastron. From this, using probabilistic considerations, they were able to derive an upper limit of $|\hat{\alpha}_1| < 5 \times 10^{-4}$ with a 90% confidence level. After the discovery of a number of new small-eccentricity binaries, Wex (2000) extended this method in statistically combining multiple systems, by this taking care of a potential selection effect when simply picking the system with the most favourable parameter combination. His analysis yielded the slightly improved limit of $|\hat{\alpha}_1| < 1.2 \times 10^{-4}$ with a 95% confidence level.

In a recent paper Bailey and Kostecký (2006) study the violation of local Lorentz invariance within an effective field theory called the standard model extension (SME). Besides a number of solar system tests, they use their formalism to investigate the measurability of SME preferred-frame effects in binary pulsars. However, as already pointed out by Bailey and Kostecký, their formalism does not account for strong field effects. In addition, as we will demonstrate in the course of this paper, their usage of the PSR B1913+16 timing results does not provide a consistent test.

In this paper we present a new method for testing preferred-frame effects related to strong gravitational fields, which uses binary pulsars with a high rate of periastron advance. Our method provides independent and simultaneous tests for both $\hat{\alpha}_1$ and $\hat{\alpha}_2$. While the tests of Damour and Esposito-Farèse (1992b) and Wex (2000), by their probabilistic considerations, can only provide upper limits for preferred-frame effects, the method introduced in this paper is even capable of detecting a preferred frame in the universe, if it exists.

We apply our new method to the PSR J0737–3039 binary pulsar system (Burgay et al. 2003; Lyne et al. 2004), which is not only the only Double Pulsar system known, but which also exhibits the highest rate of periastron advance, $\dot{\omega} = d\omega/dt$, of any binary pulsar known. The precisely measured value of $\dot{\omega} = 16.89947(68)$ deg yr⁻¹ (Kramer et al. 2006) is more than four times larger than the value measured for the Hulse-Taylor pulsar PSR B1913+16 (Weisberg & Taylor 2002). While the Double Pulsar has been used to provide the so far most stringent test of GR in the strong field regime, we show here that the large periastron advance makes it also a unique testbed to actually measure a possible violation of the Lorentz invariance for strong gravitational fields, which may occur in alternative theories of gravity.

The plan of the paper is as follows. In Section 2, based on a theory-independent framework of Will (1993), we study in full the motion of a compact binary system in theories of gravity that are non-boost-invariant. We calculate the secular evolution, caused by preferred-frame effects, for all binary parameters, in order to show that the combination of these periodic parameter changes exhibits a unique ‘signature’ of a preferred frame. In Section 3 we investigate the impact of such time-dependencies on the high-precision timing measurements of binary pulsars, and how this can be used

to either measure or constrain strong-field preferred-frame effects. In Section 4 we apply our method to the Double Pulsar to obtain limits for preferred-frame effects from this system. Finally, we present results of simulations that show how the precision of this test will improve within the next couple of years, and we investigate the possibility of combining observations of several binary pulsar systems, to obtain a full sky coverage with high sensitivity.

2 PREFERRED-FRAME EFFECTS IN THE MOTION OF COMPACT BINARIES

In this first part we study the motion of compact binary systems in theories of gravity that have a preferred frame of reference. We derive the equations of motion from a general formalism introduced by Will (1993) which includes strong field contributions using generic strong-field parameters. As we do not impose boost-invariance, the resulting equations of motion contain terms that depend on the motion of the binary system with respect to a preferred frame. Hence, our computations generalize the earlier work by Nordtvedt and Will (1972) and Damour and Esposito-Farèse (1992b) to describe binary systems and their orbital parameters with arbitrary eccentricities. Using the method of perturbations of osculating orbital elements it is shown that the rate of relativistic precession of periastron, the orbital eccentricity, and the orbital period should change in a characteristic way over time if a binary system moves relative to a preferred frame of reference.

2.1 Binary dynamics in the generalised EIH formalism

When dropping constant terms and rescaling the masses, the semi-conservative, generalised Einstein-Infeld-Hoffmann (EIH) Lagrangian of Will (1993) reads for a system consisting of two compact objects

$$L = L^{(0)} + L^{(1)}/c^2 \quad (1)$$

where

$$L^{(0)} = \frac{1}{2}m_p v_p^2 + \frac{1}{2}m_c v_c^2 + \frac{\mathcal{G}Gm_p m_c}{r} \quad (2)$$

and

$$\begin{aligned} L^{(1)} = & \frac{1}{8}\mathcal{A}_p m_p v_p^4 + \frac{1}{8}\mathcal{A}_c m_c v_c^4 \\ & + \frac{Gm_p m_c}{2r} [3\mathcal{B}(v_c^2 + v_p^2) - 7\mathcal{C}(\mathbf{v}_p \cdot \mathbf{v}_c) - \mathcal{E}(\mathbf{v}_p \cdot \hat{\mathbf{n}})(\mathbf{v}_c \cdot \hat{\mathbf{n}})] \\ & - \frac{Gm_p m_c}{2r^2} [m_p \mathcal{D}_c + m_c \mathcal{D}_p]. \end{aligned} \quad (3)$$

m_p and m_c are the inertial masses of pulsar and companion, respectively, $r = |\mathbf{r}| = |\mathbf{x}_p - \mathbf{x}_c|$ is the coordinate distance between pulsar and companion, $\hat{\mathbf{n}} \equiv \mathbf{r}/r$, \mathbf{v}_p and \mathbf{v}_c are the coordinate velocities of pulsar and companion, respectively, and G is the Newtonian constant of gravity.

The coefficients \mathcal{A}_p , \mathcal{A}_c , \mathcal{B} , \mathcal{C} , \mathcal{D}_p , \mathcal{D}_c , \mathcal{E} , and \mathcal{G} are functions of the parameters of the chosen theory of gravity and of the structure of each body. They account for contributions of the highly relativistic interior of the neutron stars to the binary dynamics. In particular, it is assumed that these coefficients are independent of the inter-

body distance in the binary system. In this paper we will denote them as ‘strong gravity coefficients’. The strong gravity coefficients \mathcal{B} , \mathcal{C} , \mathcal{E} , and \mathcal{G} are symmetric under interchange of $p \leftrightarrow c$. For instance, in the fully conservative version of Rosen’s bimetric theory $\mathcal{G} = 1 - \frac{4}{3}s_p s_c$, where s_p and s_c are the ‘first sensitivities’ ($\equiv -\partial \ln m / \partial \ln G \sim [\text{gravitational binding energy}]/[\text{mass}]$) of pulsar and companion, respectively. In GR, these parameters are unity and, therefore, the compactness of a body does not have an impact on its orbital motion, a property of GR known as the ‘effacement’ of internal structure (see the discussion in Damour 1987).

We note that combining the PFE-Terms of the Lagrangian of Damour and Esposito-Farèse (1992b) and the generalised conservative Lagrangian of Damour and Esposito-Farèse (1992a) yields a Lagrangian that is equivalent to the generalised Lagrangian of Will (1993) if one sets the \mathcal{A} -terms in Will’s Lagrangian equal to in unity. As it turns out that these \mathcal{A} -terms play an important role in the violation of Lorentz invariance, we use Will’s Lagrangian for our calculations.

In contrast to Will (1993), we do not impose post-Galilean invariance when calculating the equations of motion, in order to include gravitational theories that have a preferred frame of reference and, therefore, are not post-Galilean invariant. Hence, the equations of motion for pulsar and companion in the preferred frame are derived from the Euler-Lagrange equations

$$\frac{d}{dt} \frac{\partial L}{\partial \mathbf{v}_p} - \frac{\partial L}{\partial \mathbf{x}_p} = 0 \quad \text{and} \quad \frac{d}{dt} \frac{\partial L}{\partial \mathbf{v}_c} - \frac{\partial L}{\partial \mathbf{x}_c} = 0, \quad (4)$$

without any further restrictions on the ‘strong gravity coefficients’ of L . The relative acceleration $\mathbf{a} = \mathbf{a}_p - \mathbf{a}_c$ for a binary pulsar system at rest with respect to the preferred frame is then found to be

$$\mathbf{a} = \mathbf{a}^{(0)} + \mathbf{a}^{(1)}/c^2, \quad (5)$$

where

$$\mathbf{a}^{(0)} = -\frac{m^* \hat{\mathbf{n}}}{r^2}, \quad (6)$$

$$\begin{aligned} \mathbf{a}^{(1)} = \frac{m^* \hat{\mathbf{n}}}{r^2} \left\{ \left[1 + 3\mathcal{B}^* + (2 + \alpha_1^*) \xi_p \xi_c \right. \right. \\ \left. \left. - (1 - \mathcal{D}_c^*) \xi_p - (1 - \mathcal{D}_p^*) \xi_c \right] \frac{m^*}{r} \right. \\ \left. - \left[\frac{1}{2}(3\mathcal{B}^* - 1) + \frac{1}{2}(6 + \alpha_1^* + \alpha_2^*) \xi_p \xi_c \right. \right. \\ \left. \left. + \frac{1}{2}(1 - \mathcal{A}_c) \xi_p^3 + \frac{1}{2}(1 - \mathcal{A}_p) \xi_c^3 \right] v^2 \right. \\ \left. + \frac{3}{2}(1 + \alpha_2^*) \xi_p \xi_c (\mathbf{v} \cdot \hat{\mathbf{n}})^2 \right\} \\ + \frac{m^* \mathbf{v}}{r^2} \left[1 + 3\mathcal{B}^* - (2 - \alpha_1^* + \alpha_2^*) \xi_p \xi_c \right. \\ \left. - (1 - \mathcal{A}_c) \xi_p^3 - (1 - \mathcal{A}_p) \xi_c^3 \right] (\mathbf{v} \cdot \hat{\mathbf{n}}), \quad (7) \end{aligned}$$

where $m^* = \mathcal{G}G(m_p + m_c)$, $\xi_p = m_p/m$, $\xi_c = m_c/m = 1 - \xi_p$, $\mathcal{B}^* = \mathcal{B}/\mathcal{G}$, $\mathcal{C}^* = \mathcal{C}/\mathcal{G}$, $\mathcal{D}_p^* = \mathcal{D}_p/\mathcal{G}^2$, $\mathcal{D}_c^* = \mathcal{D}_c/\mathcal{G}^2$, $\mathcal{E}^* = \mathcal{E}/\mathcal{G}$, and further

$$\alpha_1^* = \mathcal{E}^* + 7\mathcal{C}^* - 6\mathcal{B}^* - 2, \quad (8)$$

$$\alpha_2^* = \mathcal{E}^* - 1. \quad (9)$$

Note, in GR $\alpha_1^* \equiv \alpha_2^* \equiv 0$. Further, α_1^* and α_2^* are proportional to the PFE parameters $\hat{\alpha}_1$ and $\hat{\alpha}_2$ of Damour and Esposito-Farèse (1992b), respectively: $\alpha_i^* = \mathcal{G}\hat{\alpha}_i$.

The ‘Newtonian’ part of the above equations of motion, $\mathbf{a}^{(0)}$, has the well-known Keplerian solution

$$\mathbf{r} = r(\mathbf{e}_X \cos \phi + \mathbf{e}_Y \sin \phi), \quad r = \frac{p}{1 + e \cos \phi} \quad (10)$$

$$r^2 \dot{\phi} = (m^* p)^{1/2}, \quad (11)$$

where

$$p = a(1 - e^2) \quad \text{and} \quad (P_b/2\pi)^2 = a^3/m^*. \quad (12)$$

P_b is the orbital period of the binary system and e the eccentricity of its orbit.

The post-Newtonian terms, $\mathbf{a}^{(1)}/c^2$, produce a secular advance of periastron given by

$$\langle \dot{\omega} \rangle = \frac{6\pi m^*}{c^2 p P_b} \hat{\mathcal{P}}, \quad (13)$$

where

$$\begin{aligned} \hat{\mathcal{P}} = \mathcal{B}^* + \frac{1}{6}(1 - \mathcal{D}_p^*) \xi_c + \frac{1}{6}(1 - \mathcal{D}_c^*) \xi_p \\ + \frac{1}{6}(2\alpha_1^* - \alpha_2^*) \xi_p \xi_c - \frac{1}{6}(1 - \mathcal{A}_p) \xi_c^3 - \frac{1}{6}(1 - \mathcal{A}_c) \xi_p^3. \quad (14) \end{aligned}$$

2.2 Preferred-frame effects in the relativistic binary motion

In the previous Section we have given results for a binary-pulsar system that is at rest with respect to the preferred frame of reference. In this Section we investigate the dynamics of a binary system that moves relative to the preferred frame with velocity \mathbf{w} . As a matter of convenience, we will use a frame that is comoving with the binary system. The equations of motion in the comoving frame can be derived by imposing a post-Galilean transformation (Chandrasekhar and Contopoulos 1967) on the equations of motion that result from the Euler-Lagrange equations (4) of the previous Section. For the relative acceleration, as expressed in the comoving frame, one finds

$$\mathbf{a} = \mathbf{a}^{(0)} + \mathbf{a}^{(1)}/c^2 + \mathbf{a}^{(w)}/c^2, \quad (15)$$

where

$$\begin{aligned} \mathbf{a}^{(w)} = \\ -\frac{m^* \hat{\mathbf{n}}}{2r^2} \left[\alpha_1^* (\xi_p - \xi_c) (\mathbf{w} \cdot \mathbf{v}) - 3\alpha_2^* (\mathbf{w} \cdot \hat{\mathbf{n}})^2 \right. \\ \left. + (1 - \mathcal{A}_c) \xi_p w^2 + (1 - \mathcal{A}_p) \xi_c w^2 \right. \\ \left. - (1 - \mathcal{A}_c) \xi_p^2 (\mathbf{w} \cdot \mathbf{v}) + (1 - \mathcal{A}_p) \xi_c^2 (\mathbf{w} \cdot \mathbf{v}) \right] \\ + \frac{m^* \mathbf{w}}{2r^2} \left[\alpha_1^* (\xi_p - \xi_c) (\mathbf{v} \cdot \hat{\mathbf{n}}) - 2\alpha_2^* (\mathbf{w} \cdot \hat{\mathbf{n}}) \right. \\ \left. - 2(1 - \mathcal{A}_c) \xi_p (\mathbf{w} \cdot \hat{\mathbf{n}}) - 2(1 - \mathcal{A}_p) \xi_c (\mathbf{w} \cdot \hat{\mathbf{n}}) \right. \\ \left. + 2(1 - \mathcal{A}_c) \xi_p^2 (\mathbf{v} \cdot \hat{\mathbf{n}}) - 2(1 - \mathcal{A}_p) \xi_c^2 (\mathbf{v} \cdot \hat{\mathbf{n}}) \right] \\ - \frac{m^* \mathbf{v}}{r^2} \left[(1 - \mathcal{A}_c) \xi_p^2 (\mathbf{w} \cdot \hat{\mathbf{n}}) - (1 - \mathcal{A}_p) \xi_c^2 (\mathbf{w} \cdot \hat{\mathbf{n}}) \right], \quad (16) \end{aligned}$$

The variations of the orbital parameters of a binary pulsar caused by the preferred-frame acceleration $\mathbf{a}^{(w)}/c^2$ can now be calculated by the standard technique of perturbations of osculating orbital elements. Using the notation of Damour and Taylor (1992), one finds, when averaging over

one full orbit, for the change in the longitude of periastron

$$\Delta\omega^{(w)} = \frac{\pi m^*}{c^2 p} \left[\frac{1}{2} \hat{Q}_1 \left(\frac{1}{e} - e F_e^2 \right) \left(\frac{w}{v_0} \right) \sin \psi \sin \chi - \hat{Q}_2 F_e^2 \left(\frac{w}{v_0} \right)^2 \sin^2 \psi \cos 2\chi \right] - \Delta\Omega \cos i, \quad (17)$$

for the change in the longitude of the ascending node

$$\Delta\Omega^{(w)} = \frac{\pi m^*}{c^2 p \sin i} F_e \left[\hat{Q}_1 e \left(\frac{w}{v_0} \right) \cos \psi \cos \omega - \hat{Q}_2 \left(\frac{w}{v_0} \right)^2 \sin 2\psi \left(\frac{\cos \chi \sin \omega}{\sqrt{1-e^2}} + \sin \chi \cos \omega \right) \right], \quad (18)$$

for the change in the projected semi-major axis

$$\frac{\Delta x^{(w)}}{x} = -\frac{\pi m^*}{c^2 p \tan i} F_e \left[\hat{Q}_1 e \left(\frac{w}{v_0} \right) \cos \psi \sin \omega + \hat{Q}_2 \left(\frac{w}{v_0} \right)^2 \sin 2\psi \left(\frac{\cos \chi \cos \omega}{\sqrt{1-e^2}} - \sin \chi \sin \omega \right) \right], \quad (19)$$

for the change in the eccentricity

$$\Delta e^{(w)} = \frac{\pi m^*}{c^2 p} (1+e^2) F_e \left[\hat{Q}_1 \left(\frac{w}{v_0} \right) \sin \psi \cos \chi + \hat{Q}_2 \frac{e F_e}{\sqrt{1-e^2}} \left(\frac{w}{v_0} \right)^2 \sin^2 \psi \sin 2\chi \right], \quad (20)$$

for the change in the mean anomaly (dropping terms independent of χ)

$$\Delta M^{(w)} = -\sqrt{1-e^2} \left[\Delta\omega^{(w)} + \Delta\Omega^{(w)} \cos i \right] + \frac{\pi m^*}{c^2 p} \left[12 \hat{Q}'_1 e F_e \sqrt{1-e^2} \left(\frac{w}{v_0} \right) \sin \psi \sin \chi + \hat{Q}'_2 \left(2 F_e \sqrt{1-e^2} - 1 \right) \left(\frac{w}{v_0} \right)^2 \sin^2 \psi \cos 2\chi \right], \quad (21)$$

where

$$\hat{Q}_1 = \alpha_1^* (\xi_p - \xi_c) - 2(1 - \mathcal{A}_p) \xi_c^2 + 2(1 - \mathcal{A}_c) \xi_p^2, \quad (22)$$

$$\hat{Q}_2 = \alpha_2^* + (1 - \mathcal{A}_c) \xi_p + (1 - \mathcal{A}_p) \xi_c, \quad (23)$$

$$\hat{Q}'_1 = (1 - \mathcal{A}_p) \xi_c^2 - (1 - \mathcal{A}_c) \xi_p^2, \quad (24)$$

$$\hat{Q}'_2 = \alpha_2^* - 2(1 - \mathcal{A}_c) \xi_p - 2(1 - \mathcal{A}_p) \xi_c, \quad (25)$$

and

$$F_e = \frac{1}{1 + \sqrt{1-e^2}}. \quad (26)$$

ψ is the angle between $\hat{\mathbf{k}}$, the direction of the orbital angular momentum, and \mathbf{w} . χ is the angle between the periastron of the pulsar and the projection of \mathbf{w} into the orbital plane.

In fully conservative theories of gravity one finds $\mathcal{A}_p \equiv \mathcal{A}_c \equiv 1$ and $\alpha_1^* \equiv \alpha_2^* \equiv 0$. Consequently fully conservative theories of gravity do not predict any preferred-frame effects in the motion of compact binaries, i.e. $\hat{Q}_1 = \hat{Q}_2 = \hat{Q}'_1 = \hat{Q}'_2 = 0$. In GR, in addition to the absence of preferred-frame effects, one has $\hat{P} = 1$.

2.3 The PPN limit

In the true post-Newtonian limit for masses with negligible self gravity one finds the strong gravity coefficients as functions of the PPN parameters β , γ , α_1 , and α_2 (Will 1993):

$$\mathcal{G} = 1, \quad (27)$$

$$\mathcal{A}_p = \mathcal{A}_c = 1, \quad (28)$$

$$\mathcal{B}^* = \frac{1}{3}(2\gamma + 1), \quad (29)$$

$$\mathcal{C}^* = \frac{1}{7}(4\gamma + 3 + \alpha_1 - \alpha_2), \quad (30)$$

$$\mathcal{D}_p^* = \mathcal{D}_c^* = 2\beta - 1, \quad (31)$$

$$\mathcal{E}^* = 1 + \alpha_2, \quad (32)$$

and

$$\alpha_1^* = \alpha_1, \quad (33)$$

$$\alpha_2^* = \alpha_2. \quad (34)$$

Hence

$$\hat{P} = \frac{1}{3}(2 + 2\gamma - \beta) + \frac{1}{6}(2\alpha_1 - \alpha_2) \xi_p \xi_c, \quad (35)$$

$$\hat{Q}_1 = \alpha_1 (\xi_p - \xi_c), \quad (36)$$

$$\hat{Q}_2 = \alpha_2, \quad (37)$$

$$\hat{Q}'_1 = 0. \quad (38)$$

$$\hat{Q}'_2 = \alpha_2, \quad (39)$$

Nordtvedt and Will (1972) derive the contribution of a preferred frame to the advance of periastron and the change in the eccentricity for planetary orbits (equations 61, 62). In the PPN-limit our equations (17) and (20) agree with their results if one assumes $m_p \ll m_c$ and $e \ll 1$. As we restrict our discussion to semi-conservative theories of gravity, we do not get the self-acceleration terms related to α_3 .

3 TESTING PREFERRED-FRAME EFFECTS IN BINARY PULSARS

We have seen in the previous Section that if a binary pulsar moves with respect to a preferred frame of reference, changes of its orbital parameters occur, which should then become apparent in its timing data. Therefore, assuming a direction and velocity w for the preferred frame[†] we will demonstrate that timing data can be used to constrain or even measure the strong field parameters \hat{Q}_1 and \hat{Q}_2 , which determine the strength of the preferred-frame effects.

3.1 Measuring PFE effects

Equations (17) to (21) can be converted into (averaged) first order time derivatives in the orbital elements via $\langle \dot{\omega} \rangle = \Delta\omega/P_b$, etc. At a first glance, comparing these expressions with the observed values for $\dot{\omega}$, \dot{x} , and \dot{e} [‡] obtained in timing observations, seems to provide a method to measure or at least constrain the strong-field parameters \hat{Q}_1 and \hat{Q}_2 . In particular, using a measurement for $\dot{\omega}$ seems to be very

[†] We do not make any assumption about the nature of this preferred frame in our derivation. Only later, we investigate observational data assuming some natural choices such as the motion of the binary pulsar with respect to the cosmic microwave background, representing a distinguishable frame of reference in the Universe (Nordtvedt and Will 1972).

[‡] Note that $\dot{\Omega}$ is not an observable quantity.

attractive, as this timing parameter is usually the easiest to determine among the so called ‘‘Post-Keplerian’’ parameters. However, this seemingly straightforward approach of using only the first order time derivatives has a number of problems: (a) the gravitational mass parameter m^* can usually not be determined in a theory-independent way, (b) the value of the strong-field parameter $\hat{\mathcal{P}}$ is not known, hence prevents the use of $\langle \dot{\omega} \rangle$, and (c) for the most promising test systems the orbit is usually relativistic enough to cause a non-linear evolution of the orbital parameters. We discuss each these potential problems in turn.

Without making detailed assumptions on the strong-field properties of the underlying theory of gravity, most binary pulsars will not allow the determination of m^* and the orbital inclination i as required in equations (17) to (21). Indeed, most Post-Keplerian parameters, like the Einstein delay, γ , or the change in orbital period due to gravitational wave damping, \dot{P}_b , cannot be used as they are expected to have strong-field contributions, which are not quantified within a theory-independent framework as used in this paper. In contrast, under some very natural assumptions concerning the leading terms in the space-time metric in the inter-body region and far from a binary pulsar system, the observation of a Shapiro delay can be used to determine the sine of the orbital inclination. We will discuss this point in more detail later, when we also demonstrate that under very special circumstances, such information can be used to actually determine both mass parameters $m_p^* = \mathcal{G}Gm_p$ and $m_c^* = \mathcal{G}Gm_c$.

Even if we could determine m^* from post-Keplerian parameters not involving $\dot{\omega}$, we still could not extract the preferred-frame contribution in $\langle \dot{\omega} \rangle$ as we do not have a (theory-independent) value for $\hat{\mathcal{P}}$ of equation (13). In other words, usually one cannot separate the preferred-frame terms from the other relativistic terms.

Moreover, one can precisely measure post-Keplerian parameters only in relativistic binary pulsars. In such a case, the preferred-frame effects as described by equations (17) to (21) cannot be described by a simple linear-in-time expressions, like $e = \langle \dot{e} \rangle (t - t_0)$. Fitting for first order time derivatives, therefore, cannot be used to consistently test for preferred-frame effects in these systems. This is true for any binary pulsar system where due to a relativistic advance of periastron the longitude of periastron has changed significantly since the time of its discovery. For instance, in PSR B1913+16 ω has advanced by about 135 degrees since its discovery in 1974, and therefore first order time derivatives cannot be used to constrain preferred frame effects, as done in Bailey and Kostelecký (2006). The result is a significant change in χ since $\chi = \text{const.} - \omega(t)$. Consequently, the time derivatives of the orbital parameters are trigonometric functions of $\omega(t)$ and, accordingly, the preferred-frame effects impose periodic changes on the orbital parameters themselves, with frequencies $\dot{\omega}$ and $2\dot{\omega}$.

In order to test for preferred-frame effects in such systems, one needs to include this periodic ‘signature’ of a preferred frame into the timing model, which is used for fitting the timing data. In the following we will describe a timing model and apply it to the Double Pulsar.

3.2 A timing model for the ‘signature’ of preferred-frame effects

3.2.1 Case I. $i \simeq 90$ degrees

As outlined in the previous Section, the presence of preferred-frame effects in the motion of a binary system results in periodic changes of the orbital elements. In this Section we will extend the existing standard Damour & Deruelle (DD) timing model (Damour & Deruelle 1985, 1986) to include these periodic changes and, therefore, allows to fit for the amplitudes of these preferred-frame effects. We will demonstrate our method by applying it to the Double Pulsar system, and so we restrict the following discussion to binary systems with an orbital inclination, i , close to 90 degrees. A generalisation for systems with orbital inclinations significantly less than 90 degrees is straightforward.

If $i \simeq 90^\circ$ changes in the projected semi-major axis (equation 19) are small and can be neglected in the timing model. In the following $\tilde{\chi}_0$ denotes the angle between the ascending node and the projection of \mathbf{w} into the orbital plane, \mathbf{w}_\perp , and consequently $\chi = \tilde{\chi}_0 - \omega$ (see Fig. 1).

Integrating equation (17) for $i = 90^\circ$ one finds

$$\Delta\omega^{(w)}(T) = \eta_1^{(w)} \cos(\omega_L - \tilde{\chi}_0) - \eta_2^{(w)} \sin 2(\omega_L - \tilde{\chi}_0), \quad (40)$$

where

$$\omega_L = \omega_0 + \dot{\omega}^{(1)}(T - T_0), \quad (41)$$

and

$$\eta_1^{(w)} = \frac{\hat{Q}_1}{12\hat{\mathcal{P}}} \left(\frac{1}{e} - eF_e^2 \right) \left(\frac{w}{v_0} \right) \sin \psi, \quad (42)$$

$$\eta_2^{(w)} = \frac{\hat{Q}_2}{12\hat{\mathcal{P}}} F_e^2 \left(\frac{w}{v_0} \right)^2 \sin^2 \psi. \quad (43)$$

When integrating, we have made the assumption that it is sufficient to keep terms linear in $\eta_i^{(w)}$.[§] Hence $\dot{\omega}^{(1)}$ is given by equation (13).

Integrating equation (21) one finds

$$\Delta e^{(w)}(T) = \eta_1^{(e)} \sin(\omega_L - \tilde{\chi}_0) + \eta_2^{(e)} \cos 2(\omega_L - \tilde{\chi}_0). \quad (44)$$

where

$$\eta_1^{(e)} = \frac{\hat{Q}_1}{6\hat{\mathcal{P}}} (1 + e^2) F_e \left(\frac{w}{v_0} \right) \sin \psi, \quad (45)$$

$$\eta_2^{(e)} = \frac{\hat{Q}_2}{12\hat{\mathcal{P}}} \frac{e(1 + e^2) F_e}{\sqrt{1 - e^2}} \left(\frac{w}{v_0} \right)^2 \sin^2 \psi. \quad (46)$$

Integrating equation (20) one finds

$$\Delta M^{(w)}(T) = -\eta_1^{(M)} \cos(\omega_L - \tilde{\chi}_0) + \eta_2^{(M)} \sin 2(\omega_L - \tilde{\chi}_0), \quad (47)$$

where

$$\eta_1^{(M)} = \eta_1^{(w)} \sqrt{1 - e^2} + \frac{\hat{Q}'_1}{\hat{\mathcal{P}}} e F_e \sqrt{1 - e^2} \left(\frac{w}{v_0} \right)^2 \sin^2 \psi, \quad (48)$$

$$\eta_2^{(M)} = \eta_2^{(w)} \sqrt{1 - e^2} + \frac{\hat{Q}'_2}{6\hat{\mathcal{P}}} \left(F_e \sqrt{1 - e^2} - \frac{1}{2} \right) \left(\frac{w}{v_0} \right)^2 \sin^2 \psi. \quad (49)$$

[§] It can be verified directly by fitting the timing data if this assumption is applicable.

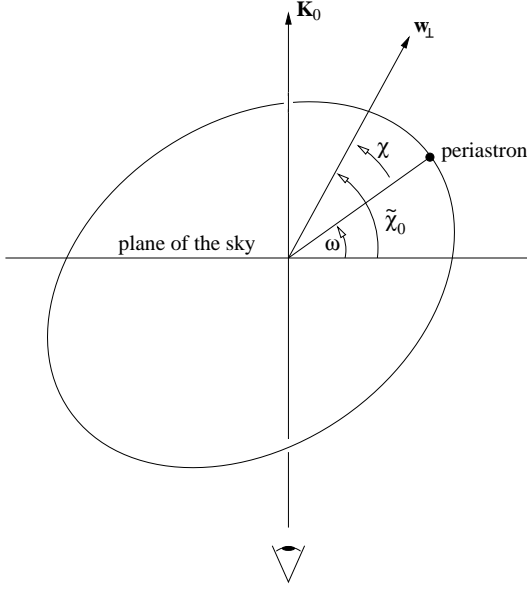


Figure 1. Definition of angles in the PFE timing model.

We emphasize that the ratios $\eta_1^{(\omega)}/\eta_1^{(e)}$ and $\eta_2^{(\omega)}/\eta_2^{(e)}$ are only functions of the Keplerian eccentricity, e , of the binary system.

For a consistent, theory-independent analysis of binary pulsar timing data, Damour and Deruelle developed a phenomenological timing model, using a parametrized post-Keplerian approach (Damour & Deruelle 1985, 1986). The DD timing model applies to the class of Lorentz-invariant theories of gravity, such as the well-motivated tensor-scalar theories. However, it does not describe the preferred-frame effects that we consider here. On the other hand, it is easy to incorporate these variations into the DD timing model by simply adding solutions (40), (44), (47) accordingly to the the DD model:

$$\omega(T) \rightarrow \omega(T) + \Delta\omega(T)^{(\omega)}, \quad (50)$$

$$e(T) \rightarrow e(T) + \Delta e(T)^{(\omega)}, \quad (51)$$

$$\frac{2\pi}{P_b}(T - T_0) \rightarrow \frac{2\pi}{P_b}(T - T_0) + \Delta M(T)^{(\omega)}. \quad (52)$$

Therefore our new timing formula, for binary pulsars with $i \simeq 90^\circ$, contains, in addition to the Keplerian and post-Keplerian parameters of the DD timing model, five new preferred-frame timing parameters: the four PFE amplitudes $\eta_1^{(\omega)}$, $\eta_2^{(\omega)}$, $\eta_1^{(M)}$, $\eta_2^{(M)}$, and the angle $\tilde{\chi}_0$. The amplitudes $\eta_1^{(e)}$ and $\eta_2^{(e)}$ are proportional to $\eta_1^{(\omega)}$ and $\eta_2^{(\omega)}$ respectively, where the factors are only functions of the Keplerian eccentricity, e .

If the longitude of periastron has advanced for a considerable amount ($\gtrsim 90^\circ$) since the discovery of a binary pulsar, the timing data will allow to fit for all of these new timing parameters. If the binary motion shows the effect of a preferred-frame in the Universe, all five independent ‘preferred-frame parameters’, $\eta_1^{(\omega)}$, $\eta_2^{(\omega)}$, $\eta_1^{(M)}$, $\eta_2^{(M)}$, and $\tilde{\chi}_0$ can be determined. One can even decide to fit additionally for $\eta_1^{(e)}$ and $\eta_2^{(e)}$ i.e. perform a fit simultaneously for these parameters and for $\eta_1^{(\omega)}$ and $\eta_2^{(\omega)}$. The existence of a preferred frame could then be confirmed by verifying the expected relationship between the PFE amplitudes in ω and e . The

ratios of these amplitudes are unique in the sense that they are a function of e only and therefore independent of any strong-field parameters, and of the magnitude and direction of \mathbf{w} . For the parameters of the Double Pulsar we would expect to measure

$$\eta_1^{(\omega)}/\eta_1^{(e)} = 11.262, \quad (53)$$

$$\eta_2^{(\omega)}/\eta_2^{(e)} = 5.642 \quad (54)$$

if a preferred frame exists. This first test would incontrovertibly reveal the existence of a preferred frame. We will show later, how the direction of the preferred can also be constrained or even determined.

In the absence of any preferred-frame effect, we expect none of the PFE timing parameters to have significant values. In particular, the magnitude of PFE amplitudes should be consistent with zero, and the angle $\tilde{\chi}_0$ is undefined. In this case, one can obtain upper and lower limits for $\eta_1^{(\omega)}$, $\eta_2^{(\omega)}$, $\eta_1^{(M)}$, and $\eta_2^{(M)}$ by holding $\tilde{\chi}_0$ fixed to a particular value while fitting for the PFE amplitudes. Stepping through the possible values $\tilde{\chi}_0 \in [0, 2\pi]$, various directions on the sky can be probed. In the case of a relativistic binary pulsar, a clear separation of the preferred-frame contribution ($\eta_1^{(\omega)}$, $\eta_2^{(\omega)}$) from the other relativistic terms ($\dot{\omega}^{(1)}$) in the precession of periastron is possible and will improve with time due to increasing coverage of ω -space.

3.2.2 Case II. $i \neq 90$ degrees

As stated earlier, the above assumes that $i \simeq 90^\circ$. If one allows for any orbital inclinations, one finds that equation (40) is replaced by

$$\Delta\omega = \eta_1^{(\omega)'} \cos(\omega_L - \tilde{\chi}_0 + \delta_1') - \eta_2^{(\omega)'} \sin 2(\omega_L - \tilde{\chi}_0 + \delta_2'). \quad (55)$$

Like $\eta_1^{(\omega)}$ and $\eta_2^{(\omega)}$, $\eta_1^{(\omega)'}$ and $\eta_2^{(\omega)'}$ are proportional to \hat{Q}_1/\hat{P} and \hat{Q}_2/\hat{P} respectively, while δ_1' and δ_2' depend only on Keplerian parameters and the orientation of the pulsar with respect to the preferred frame. In this case also $x(T)$ has to be considered, for which one finds an expression similar to equation (55). Following the procedure above, a derivation of these expressions is straight forward.

3.3 Translating timing model parameters to strong-field PFE parameters

In this Section we give a description on how to convert the timing results, obtained after applying the new *PFE timing model*, into the strong-field PFE parameters introduced in Section 2.

As discussed in the previous Section, for a binary pulsar with $i \simeq 90^\circ$ values for the timing parameters $\eta_1^{(\omega)}$, $\eta_2^{(\omega)}$, $\eta_1^{(M)}$, and $\eta_2^{(M)}$ can be converted into values for $\hat{Q}_1 w \sin \psi / \hat{P}$, $\hat{Q}_2 w^2 \sin^2 \psi / \hat{P}$, $\hat{Q}_1' w \sin \psi / \hat{P}$, $\hat{Q}_2' w^2 \sin^2 \psi / \hat{P}$. Without any further assumptions, however, we cannot determine or even restrict the angle ψ . Here one has to keep in mind that, in general, the longitude of the ascending node of the pulsar orbit, Ω , cannot be determined from pulsar timing observations and has to be treated as a free parameter. We discuss possible exceptions further below.

Relating the orientation of the orbit to the movement relative to a preferred frame in direction \mathbf{w} , requires the

knowledge of the orbital inclination angle. In cases where the binary orbit is seen nearly edge-on, one can often determine this angle accurately, as one expects to observe an additional delay in the arrival time of the pulsar signal during superior conjunction of the pulsar, caused by the gravitational field of the companion. This is the case in the Double Pulsar where this ‘‘Shapiro effect’’ can be used to determine the orbital inclination i (modulo the ambiguity $i \rightarrow \pi - i$). In order to do this, one only have to make some general, very natural assumptions. As in Will (1993), we assume that to first order the metric valid in the inter-body region and far from the system can be written as

$$g_{00} = -1 + \frac{2G\kappa_p^* m_p}{c^2 |\mathbf{x} - \mathbf{x}_p|} + \frac{2G\kappa_c^* m_c}{c^2 |\mathbf{x} - \mathbf{x}_c|} \quad (56)$$

$$g_{0j} = 0 \quad (57)$$

$$g_{ij} = \left(1 + \frac{2G\gamma_p^* m_p}{c^2 |\mathbf{x} - \mathbf{x}_p|} + \frac{2G\gamma_c^* m_c}{c^2 |\mathbf{x} - \mathbf{x}_c|} \right) \delta_{ij} \quad (58)$$

where κ_p^* , γ_p^* , κ_c^* , and γ_c^* are functions of the parameters of the theory and of the structure of pulsar and companion. In GR $\kappa_p^* = \gamma_p^* = \kappa_c^* = \gamma_c^* = 1$. The time taken by the pulsar signal to travel from the pulsar to the solar system in such a metric can be accounted for by adding

$$\Delta_S = \frac{G(\kappa_c^* + \gamma_c^*)m_c}{c^3} \ln \left\{ 1 - e \cos U \right. \\ \left. - \sin i \left[\sin \omega (\cos U - e) \right. \right. \\ \left. \left. + (1 - e^2)^{1/2} \cos \omega \sin U \right] \right\}. \quad (59)$$

to the timing model, which can be used to fit for $\sin i$, the ‘‘shape’’ of the Shapiro delay, without any knowledge of the strong-field parameters (Blandford and Teukolsky 1976, Damour and Deruelle 1986b, Will 1993). U is the eccentric anomaly as defined by the DD model. The measurement of $\sin i$ then allows to exclude certain directions of \mathbf{w} in the sky, given certain values of $\tilde{\chi}_0$. In fact, if one makes certain assumptions of the magnitude and direction of \mathbf{w} , i.e. the direction and motion of the preferred frame, a measurement of $\sin i$ (and the computation of $\tilde{\chi}_0$) will allow the determination of $\sin \psi$, and, consequently, the determination of \hat{Q}_1/\hat{P} and \hat{Q}_2/\hat{P} for the assumed preferred frame from the fitted PFE amplitudes.

On the other hand, as outlined earlier, if no preferred-frame effects are observable in the orbital motion of a binary pulsar, fitting for the PFE amplitudes (while holding $\tilde{\chi}_0$ fixed) can be used to determine limits on $\hat{Q}_1 w/\hat{P}$, $\hat{Q}_2 w^2/\hat{P}$, $\hat{Q}'_1 w/\hat{P}$, and $\hat{Q}'_2 w^2/\hat{P}$ for (nearly) any direction in the sky. However, during this transformation from PFE timing model parameters to these physical quantities, one needs to determine $\tilde{\chi}_0$ and ψ for a given direction in the sky. That requires the knowledge of the, in general, unknown angle Ω , while one also has to account for the ambiguity in the sense of the inclination i . Two practical approaches exist to overcome this problem. These angles can either be chosen such that the limits are most conservative, or one can perform Monte-Carlo simulations varying over Ω and the two possible values for i . Assuming a uniform distribution for Ω and equal probability for i and $\pi - i$, it is possible to determine limits for any chosen confidence level. It is clear that the most conservative method cannot provide any restrictions for directions along a cone that has an opening angle

i around the line of sight, as for any direction on this cone, Ω can be chosen such that $\psi = 0$.

The situation is obviously improved if Ω can be determined. We note that the proper motion of a binary pulsar can produce secular changes in the orbital elements that depend on the longitude of the ascending node, Ω , and the orbital inclination, i , as it changes the apparent geometrical orientation of the orbit (Arzoumanian et al. 1996 and Kopeikin 1996). In principle these changes can be used to determine Ω and i from timing observations. However, in practice it will be difficult to separate the proper motion effects from the relativistic changes of the binary orbit, in particular if we make only very generic assumptions about the underlying theory of gravity, as we do in this paper.

In principle, measurements of the timescale of the interstellar scintillation (ISS) over an orbit can also be used to estimate the orbital inclination i and the transverse velocity of the centre of mass of the system (Lyne & Smith 1982, Ransom et al. 2004, Coles et al. 2005). A comparison of the transverse velocity derived from ISS and the transverse velocity obtained from timing observation could then be used to determine Ω . However, the scintillation-based velocity depends on a number of assumptions about the properties of the effective scattering screen and, therefore, are more susceptible to systematic errors than timing measurements.

4 THE DOUBLE PULSAR

Following the discovery of the Double Pulsar system in April 2003 (Burgay et al. 2003; Lyne et al. 2004), timing observations have enabled the most stringent tests of GR in the strong-field regime to date (Kramer et al. 2006). Indeed, the system is a unique laboratory for gravitational physics for a number of reasons. Firstly, both members of the binary system are visible as active radio pulsars, providing access to a simple measurement of the ratio of their masses and hence providing theory-independent (at least to 1PN order) constraints for tests of theories of gravity.

Secondly, the fortunate orientation of the binary orbit in space allows us to observe the Double Pulsar under a nearly perfect edge-on geometry. In addition to precise measurements of a Shapiro delay, this enables further independent estimates of the system’s inclination angle. ¶

The combination of the determination of $\sin i$ via the Shapiro delay with the measurement of the mass ratio allows a theory-independent determination of both mass parameters, m_p^* and m_c^* , as we will discuss in detail later. In this case \hat{P} can now be measured independently, thus directly giving limits for \hat{Q}_1 and \hat{Q}_2 from fitting for $\eta_1^{(\omega)}$ and $\eta_2^{(\omega)}$. Further, from this one can determine α_1^* and α_2^* for gravity theories that fulfil $\mathcal{A}_p \equiv \mathcal{A}_c \equiv 1$. In this sense the Double Pulsar is indeed a unique laboratory for strong-field preferred-frame effects.

¶ Observations and modelling of the eclipse of the radio emission of the millisecond pulsar PSR J0737–3039A during superior conjunction, lasting for about 25–30 seconds, provides another estimate (Breton et al. 2006), while two methods using observed scintillation properties provide two others (Ransom et al. 2004; Coles et al. 2005).

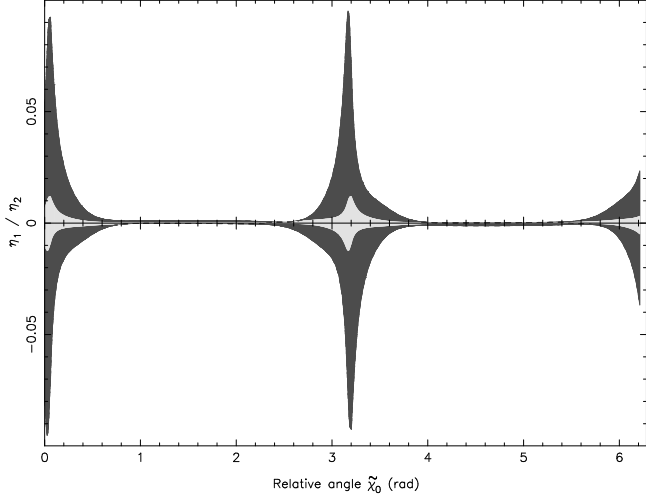


Figure 2. Limits on the existence of preferred-frame effects present in the orbital motion of the Double Pulsar as measured by the parameters $\eta_1^{(\omega)}$ (dark grey) and $\eta_2^{(\omega)}$ (light grey) as introduced in the PFE timing model. See text for details.

The third reason why the Double Pulsar is a unique gravity lab is the compactness of the orbit. With larger mean orbital velocities than in any other binary pulsar, the system is the most relativistic system known. This is reflected by the measurement of the largest advance of periastron observed in any binary system. As a result, the Double Pulsar orbit precesses by 16.9 degrees per year with respect to any possible existing preferred frame, changing the angle χ in Fig. 1 by a corresponding amount. As such the Double Pulsar is an ideal candidate to study the existence of preferred-frame effects in strong-field gravity as the magnitude of ω does not only allow its very precise measurement (currently at the 4×10^{-5} level) but the orbit also ‘covers’ a lot of periastron angle space in a rather short time span. According to the theoretical framework laid out in the previous sections, such a system is ideal for testing for PFE variations in the orbital parameters, the ‘signature’ of a preferred frame.

4.1 Application of the PFE timing model

In Section 3, we have developed the *PFE timing model* that introduces, based on the DD timing model, the new PFE model parameters $\eta_1^{(\omega)}$, $\eta_1^{(M)}$, $\eta_2^{(\omega)}$, $\eta_2^{(M)}$, $\tilde{\chi}_0$. We now want to apply this model to the timing data of the Double Pulsar. We make use of nearly three years of timing data obtained by Kramer et al. (2006) during which the pulsar periastron has advanced by about 50 degrees.

At present the timing data of the Double Pulsar system does not show a PFE ‘signature’. Hence, we can use the data only to derive limits for the PFE amplitudes by fitting for the PFE amplitudes while holding $\tilde{\chi}_0$ fixed at a given value. We then vary $\tilde{\chi}_0$ in sufficiently small steps between 0 and 360° to derive limits for any value of $\tilde{\chi}_0$. Fig. 2 illustrates the 95% confidence for $\eta_1^{(\omega)}$ and $\eta_2^{(\omega)}$, consistent with the non-existence of preferred frames.

In principle, we would also aim to fit for $\eta_1^{(M)}$ and $\eta_2^{(M)}$ which would yield limits for \hat{Q}'_1 and \hat{Q}'_2 , giving separate limits for α_1^* , α_2^* , \mathcal{A}_p , \mathcal{A}_c when combined with the results for

$\eta_1^{(\omega)}$ and $\eta_2^{(\omega)}$. However, the Double Pulsar timing data used in this paper do not yet allow to fit for $\eta_1^{(M)}$ and $\eta_2^{(M)}$. The periastron has not advanced far enough to separate these PFE amplitudes from other orbital parameters, in particular the decrease in the orbital period due to the emission of gravitational waves. As we will show later, with longer time-spans and more coverage of the periastron angle, such a fit will be possible, while simultaneously the amplitude of all limits will be greatly reduced. It is obvious that some orientations of the orbit with respect to \mathbf{w} lead to better constraints than others.

4.2 Determination of quantitative limits

In this Section we translate the limits on the ‘signature’ of a preferred frame into quantitative limits within the generalised EIH formalism. Our goal is, first, to determine limits for $\hat{Q}_1 w$ and $\hat{Q}_2 w^2$ for any direction in the sky, and secondly, to determine limits for \hat{Q}_1 and \hat{Q}_2 for a preferred frame that is at rest with respect to the CMB and one that is at rest with respect to our galaxy.

The first step is to determine the masses from the timing data described by applying the PFE timing model. Equation (59) can be used to convert the measurement of the Shapiro “shape” timing parameter into a measurement of $\sin i$. Now, combining equation (3.15) of Damour and Taylor (1992)^{||} with the measurement of the mass ratio obtained from R in the Double Pulsar, we obtain the following values

$$m_p^* = \mathcal{G}Gm_p = (1.339 \pm 0.002) \times GM_\odot, \quad (60)$$

$$m_c^* = \mathcal{G}Gm_c = (1.250 \pm 0.002) \times GM_\odot. \quad (61)$$

It is at this point where we exploit the uniqueness of the Double Pulsar which provides us with measurements of m_p^* and m_c^* . Combining these with the observed rate of periastron advance allows us to determine the strong-field parameter $\hat{\mathcal{P}}$ (see equation 13). The result is

$$\hat{\mathcal{P}} = 1.000 \pm 0.001. \quad (62)$$

In order to establish the absolute orientation of the binary system in space, one needs the orientation of the ascending node Ω , which is still unknown for the Double Pulsar (but see discussion in Section 3). As described earlier, we perform Monte-Carlo simulations and vary this parameter between 0 and 2π for any given direction of \mathbf{w} . For a given \mathbf{w} and a given Ω , we compute the angle $\tilde{\chi}_0$ and read off the corresponding limits for $\eta_1^{(\omega)}$ and $\eta_2^{(\omega)}$ from the calculated and tabulated values shown in Fig. 2. To account also for the ambiguity in the sense of the inclination i , the whole procedure is performed for 10,000 datasets for each direction in the sky and inclination angles of i and $\pi - i$. As discussed earlier, the obtained values for $\eta_1^{(\omega)}$ and $\eta_2^{(\omega)}$ can be translated into limits for $\hat{Q}_1 w$ and $\hat{Q}_2 w^2$ using equations (42) and (43). Figs. 3 give the results of our numerical simulations for preferred frames associated with different directions of the sky as seen from the Double Pulsar. The limits shown as a colour map are derived for an assumed binary pulsar velocity relative to the preferred frame of 100 km/s. Results

^{||} Note that the effective gravitational constant \mathcal{G} in Damour and Taylor (1992) corresponds to $\mathcal{G}G$ in this paper.

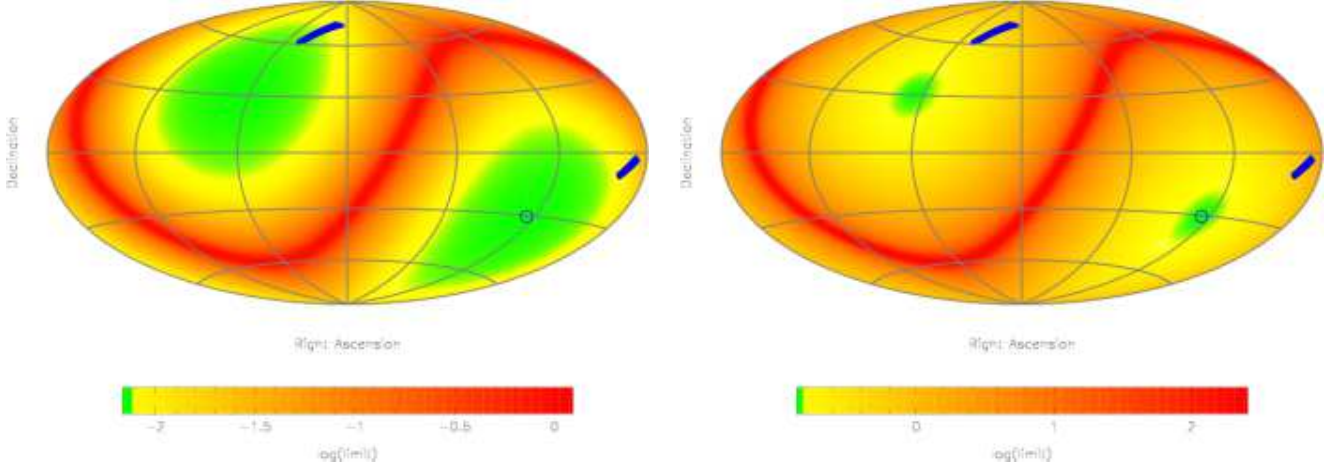


Figure 3. Limits computed for 95% confidence levels on $|Q_1|$ and $|Q_2|$ for the sky as seen by the Double Pulsar. The limits are calculated for $|\mathbf{w}| = 100$ km/s, and have to be scaled accordingly for other values of $|\mathbf{w}|$. Directions discussed in the text are marked by the blue area, i.e. direction relative to a Galactic frame (top left) and direction relative to the Cosmic Microwave Background (CMB) (right). The extension of these areas reflects the uncertainty in the radial velocity of the binary pulsar system with respect to the solar system. When extracting the limits for the Galactic and the CMB frame from these figures, one needs to keep in mind that the $|\mathbf{w}|$ of these frames changes across these areas. The location of the Sun as seen from the Double Pulsar is marked by \odot .

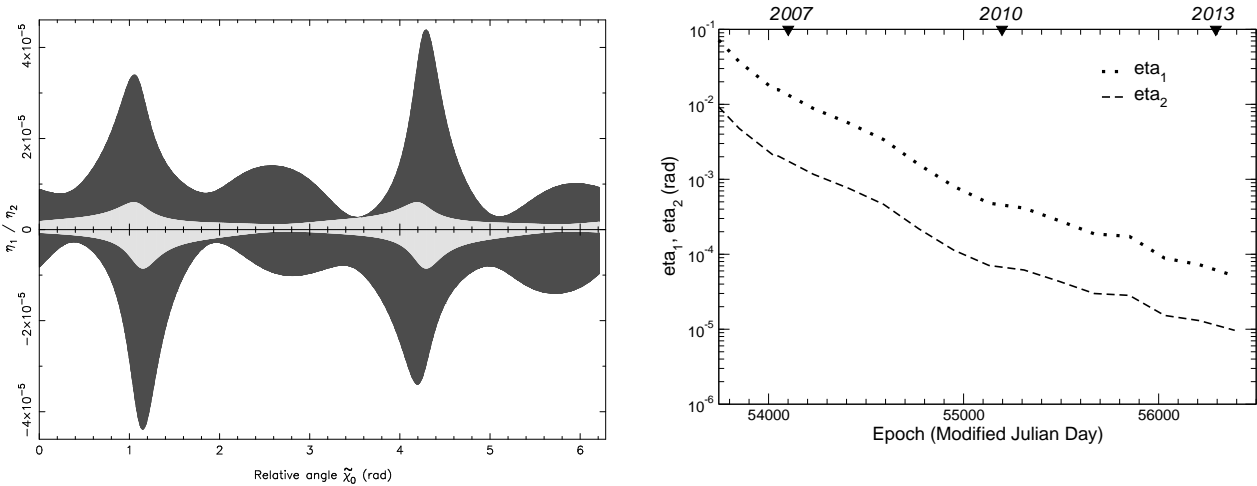


Figure 4. Future improvement of PFE tests in the Double Pulsar. (Left) Amplitude of the PFE parameters $\eta_1^{(\omega)}$ (dark grey) and $\eta_2^{(\omega)}$ (light grey) as expected for 10 years of Double Pulsar timing data. (Right) Evolution of limits on $\eta_1^{(\omega)}$ and $\eta_2^{(\omega)}$ as a function of time by recording their worst values over all χ_0 at a given epoch. The year of observation is indicated at the top of the figure.

for other relative speeds can be scaled according to equations (42) and (43).

We also indicate the directions for two selected frames that may be considered as being related to a preferred frame; we indicate the direction of motion relative to the CMB and the direction of the motion relative to the Galactic reference frame. The motion of the solar system with respect to the CMB we take from Hinshaw et al. (2006) and Lineweaver et al. (2006), and with respect to the Galactic reference frame from Mignard (2000). To calculate the motion of the Double Pulsar with respect to these frames of reference we need to know the motion of the Double Pulsar with respect to the solar system. While a proper motion of the pulsar has been measured, one of the few unknown system parameters is the

undetermined radial velocity of the system. In accordance with recent evolution studies of the Double Pulsar system (Stairs et al. 2006), we perform our analysis for a range of radial velocities between -100 and $+100$ km/s, and therefore, the direction relative to the CMB and the Galactic frame convert into small areas on the sky, from which we pick the worst 95% C.L. limits on \hat{Q}_1 and \hat{Q}_2 :

$$\text{CMB: } -0.02 < Q_1 < 0.01 \quad -0.3 < Q_2 < 0.2 \quad (63)$$

$$\text{GAL: } -0.01 < Q_1 < 0.01 \quad -0.3 < Q_2 < 0.3 \quad (64)$$

For gravity theories with $\mathcal{A}_p \equiv \mathcal{A}_c \equiv 1$ we obtain directly limits for α_1^* and α_2^* (see equations 22 and 23):

$$\text{CMB: } -0.5 < \alpha_1^* < 0.3 \quad -0.3 < \alpha_2^* < 0.2 \quad (65)$$

$$\text{GAL: } -0.3 < \alpha_1^* < 0.3 \quad -0.3 < \alpha_2^* < 0.3 \quad (66)$$

The limits given here are not very tight yet. In fact, they are several orders of magnitude worse than the limits for the weak-field PPN parameters α_1 and α_2 . On one hand, as we will discuss below, these limits will improve considerably during the next couple of years. On the other hand, these limits hold for preferred-frame effects related to strong gravitational fields. If one expands, for instance, α_1^* as a function of the sensitivity of the gravitation body

$$\alpha_1^* = \alpha_1 + \alpha_{11}(s_p + s_c) + \dots \quad (67)$$

one sees that tests in the solar system made to restrict α_1 , can only test terms which are not related to the internal gravitational fields of a body. Testing these strong-field coefficients, like α_{11} , has to be done via binary pulsars.

Our strong-field limit for α_1^* has to be compared with the limits obtained by Damour and Esposito-Farèse (1992b) and Wex (2000), which are better by about three orders of magnitude. However, in a few years from now we expect the limits obtained from the Double Pulsar to be comparable with the limits obtained from small-eccentricity binary pulsars, and as outlined in Section 3 the method presented here does not need to rely on probabilistic considerations.

Emphasizing the arguments and results presented by Will (1993) and Damour and Esposito-Farèse (1996a), we point out that Double Neutron star Systems (DNSs) are particularly sensitive to theories of gravity where higher order terms in Eqn. (67) become important, so that for instance $\alpha_1^* \propto s_p s_c$ (similarly, $\alpha_2^* \propto s_p s_c$), since for a white dwarf $s_{\text{WD}} \lesssim 10^{-3} \ll s_{\text{NS}}$.

4.3 Future measurements

The continuing precession of periastron in the Double Pulsar will lead to a constant improvement in the limits on preferred frames using our proposed method. In order to predict the future limits we have simulated timing data for the Double Pulsar, assuming similar timing precision and frequencies of observations as described in Kramer et al. (2006). Simulating data until 2013, hence for 10 years after the discovery of the system and half of the periastron precession period, we have computed the limits on the observed parameters $\eta_1^{(\omega)}$ and $\eta_2^{(\omega)}$ as a function of time. In these simulations we make the unlikely and hence conservative assumption that the timing precision will fail to improve over the next years, so that the quoted limits should be considered as conservative also. The result is shown in Fig. 4. Both parameters scale essentially similarly, and in 2013 the limits will have improved by more than two orders of magnitude, resulting in limits of $|\alpha_1^*| < 2 \times 10^{-3}$ and $|\alpha_2^*| < 2 \times 10^{-3}$. The vast improvement is also demonstrated by comparing Figure 2 with the left part of Figure 4 where we plot the limits on $\eta_1^{(\omega)}$ and $\eta_2^{(\omega)}$ as a function of $\tilde{\chi}_0$ as expected for the year 2013. These predicted values are still somewhat worse than those derived by Damour and Esposito-Farèse (1992b) and Wex (2000), but we estimate that with the timing precision being certain to improve over the next few years (e.g. by using the telescopes to be constructed as pathfinders to the Square-Kilometre Array (SKA)), the limits will be improved upon further.

In addition, by 2013 the periastron will have advanced

by nearly π since the pulsar discovery, which should also allow a separate measurement of $\eta_1^{(M)}$ and $\eta_2^{(M)}$ with comparable precision. This will provide us with measurements for \hat{Q}_1 , \hat{Q}_2 , \hat{Q}'_1 , and \hat{Q}'_2 , and consequently with values for the strong-field parameters α_1^* , α_2^* , \mathcal{A}_p , and \mathcal{A}_c .

5 AN PFE ANTENNA ARRAY

In the future, further binary systems with a variety of orientations in space will be discovered. In particular, with the Square-Kilometre Array (SKA) we expect to find about 100 relativistic DNSs (Cordes et al. 2004; Kramer et al. 2004). Some of these new systems will also be suitable sources for tests of local Lorentz-invariance of gravity, so that their observations can be combined to derive further constraints, as also pointed out by Bailey and Kostelecký (2006). Indeed, the sensitivity of additional systems to different directions in the sky will differ from that of the Double Pulsar, so that we can construct a dense network of antennae for studies of preferred-frame effects. This results in a smooth and high sensitivity toward preferred-frame effects over the whole sky.

In order to demonstrate this idea, we have simulated timing data for the Double Pulsar system if it were located at a different position in the sky, namely the Galactic Centre. Such a system would be sensitive to directions which complement those of the real Double Pulsar. This can be seen in Figure 5 where we show this situation simulated for the timing data as expected in 2013. Comparing the left panel of this figure with Figure 3 again demonstrates the vast improvement in the PFE limits over the next five to seven years. The impact of the artificial system's different position in the sky is clear from a comparison of the left and middle panel. A combination of the two sets of limits for any given direction in the sky, as shown in the right panel, demonstrates the concept of a PFE antenna array.

We point out that for tests of the most general theories only data from systems with a similar combination of pulsar and companion mass can be combined. This becomes clear when considering that the parameters \mathcal{Q}_1 and \mathcal{Q}_2 contain an explicit and implicit dependence on the neutron star masses. The implicit dependence arises from the fact that the involved strong-field coefficients are functions of the compactness of the bodies and hence of the masses and the equation-of-state of the neutron stars.

If preferred-frame effects are indeed present in the timing data of a number of binary pulsars, this array of pulsars could then be used to significantly restrict or even determine the direction of the preferred frame (modulo π related to a change of the sign in the measured PFE amplitudes), as a measurement of $\tilde{\chi}_0$ in one such system excludes the direction to lie within a cone with opening angle $\pi/2 - \tilde{\chi}_0$ around the line-of-sight to the pulsar.

6 SUMMARY

We have developed a consistent methodology to measure preferred-frame effects (PFE) related to the strong internal gravitational fields in relativistic binary pulsars. We made only very general assumptions about the underlying theory of gravity by using the semi-conservative generalised EIH

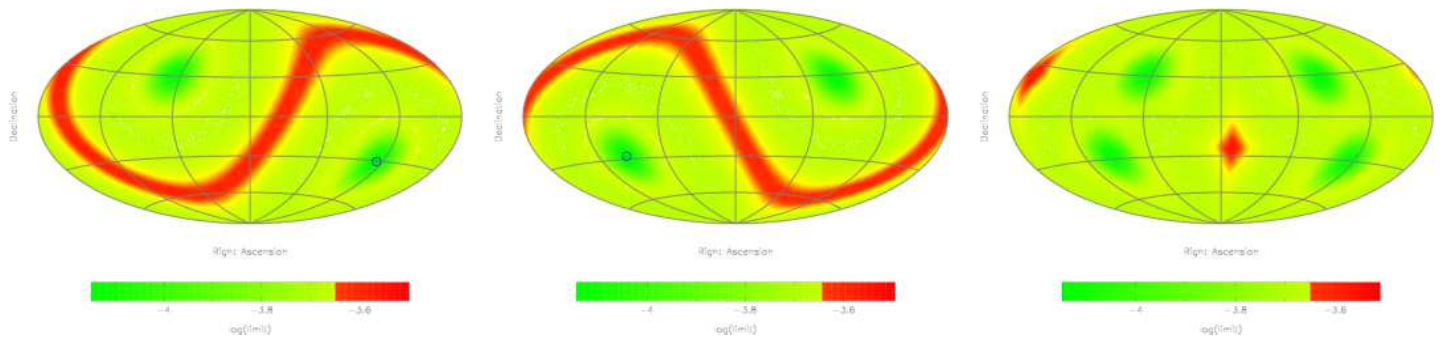


Figure 5. Limits computed for 95% confidence limits on $|Q_1|$ and $|Q_2|$ for the sky as seen by the Double Pulsar in 2013 (left) and a simulated Double Pulsar-like system located in the Galactic Centre (middle). Combining the independent constraints provided by the two systems (right) makes this PFE antenna array sensitive to most directions in the sky. For simplicity we have assumed that the two systems have a negligible relative velocity when combining the two data sets. It is clear that the addition of further systems will lead to a smooth coverage of the whole sky.

formalism of Will, which incorporates strong field effects in the post-Newtonian motion of binary pulsars. We were able to show that in relativistic binary systems with a high rate of advance of periastron, a preferred frame will cause distinctive periodic changes in the orbital elements of the binary system.

The newly developed PFE timing model extends the DD timing model by including these periodic changes, and thus having the amplitudes of these changes as additional timing parameters. We described in detail how the measurement of such PFE amplitudes can be converted into measurements of the strong field parameters related to preferred-frame effects.

For inclination angles $i \simeq 90^\circ$, the PFE amplitudes for changes in the longitude of periastron and the eccentricity are related by a factor which is independent of strong field parameters and parameters related to the preferred frame. This can be seen as a unique “fingerprint” of a preferred frame.

We have also shown that in the absence of preferred-frame effects, our formalism can be used to determine limits for these amplitudes, by this restricting the strong field parameters related to the violation of the Lorentz invariance for nearly any direction in the sky. We demonstrated that the Double Pulsar is the ideal test system for preferred-frame effects in strong gravitational fields, and have presented first preliminary results, which however are clearly less stringent than present limits from small-eccentricity binary pulsars. On the other hand, simulations show that in the next couple of years the precision of these tests will increase by several orders of magnitude. The combination of several such systems in a *PFE antenna array* for the detection of PFE effects can be used to obtain a full sky coverage.

ACKNOWLEDGEMENTS

We thank Ingrid Stairs, Dick Manchester, Maura McLaughlin, Andrew Lyne, Rob Ferdman, Marta Burgay, Duncan Lorimer, Andrea Possenti, Nichi D’Amico, John Sarkissian, George Hobbs, John Reynolds, Paulo Freire and Fernando Camilo for the collaboration on the Double Pulsar. We thank Thibault Damour for many useful and stimulating discussions, and we are in particular grateful for his comments on

the manuscript. It is also a pleasure to thank Gilles Esposito-Farèse for useful comments.

REFERENCES

- Arzoumanian Z., Joshi K., Rasio F., Thorsett S. E., 1996, in Johnston S., Walker M. A., Bailes M., eds, Pulsars: Problems and Progress, IAU Colloquium 160. Astronomical Society of the Pacific, San Francisco, p. 525
- Bailey Q. G., Kostelecký V. A., 2006, Phys. Rev. D, 74(4), 045001
- Blandford R., Teukolsky S. A., 1976, ApJ, 205, 580
- Bretton R. P. et al., 2006, On the Present and Future of Pulsar Astronomy, 26th meeting of the IAU, Joint Discussion 2, 16-17 August, 2006, Prague, Czech Republic, JD02, #21, 2
- Burgay M. et al., 2003, Nature, 426, 531
- Chandrasekhar S., Contopoulos G., 1967, Proc. Roy. Soc. (London), 298A, 123
- Coles W. A., McLaughlin M. A., Rickett B. J., Lyne A. G., Bhat N. D. R., 2005, ApJ, 623, 392
- Cordes J. M., Kramer M., Lazio T. J. W., Stappers B. W., Backer D. C., Johnston S., 2004, New Astronomy Review, 48, 1413
- Damour T., 1987, in Hawking S., Israel W., eds, 300 Years of Gravitation. Cambridge University Press
- Damour T., Deruelle N., 1985, Ann. Inst. H. Poincaré (Physique Théorique), 43, 107
- Damour T., Deruelle N., 1986, Ann. Inst. H. Poincaré (Physique Théorique), 44, 263
- Damour T., Esposito-Farèse G., 1992a, Classical and Quantum Gravity, 9, 2093
- Damour T., Esposito-Farèse G., 1992b, Phys. Rev. D, 46, 4128
- Damour T., Esposito-Farèse G., 1993, Phys. Rev. Lett., 70, 2220
- Damour T., Esposito-Farèse G., 1996a, Phys. Rev. D, 53, 5541
- Damour T., Esposito-Farèse G., 1996b, Phys. Rev. D, 54, 1474
- Damour T., Taylor J. H., 1992, Phys. Rev. D, 45, 1840
- Hinshaw G. et al., 2006, submitted to ApJ, astro-ph/0603451
- Kopeikin S. M., 1996, ApJ, 467, L93
- Kramer M., Backer D. C., Cordes J. M., Lazio T. J. W., Stappers B. W., Johnston S., 2004, New Astronomy Review, 48, 993
- Kramer M. et al., 2006, Science, 314, 97
- Lineveaver C. H., Tenorio L., Smoot G. F., Keegstra P., Banday A. J., Lubin P., 1996, ApJ, 470, 38
- Lyne A. G., Smith F. G., 1982, Nature, 298, 825
- Lyne A. G. et al., 2004, Science, 303, 1153
- Mignard F., 2000, A&A, 354, 522
- Nordtvedt K., Will C. M., 1972, ApJ, 177, 775

- Ransom S. M., Kaspi V. M., Ramachandran R., Demorest P.,
Backer D. C., Pfahl E. D., Ghigo F. D., Kaplan D. L., 2004,
ApJ, 609, L71
- Stairs I. H., 2003, Living Reviews in Relativity, 6, 5
- Stairs I. H., Thorsett S. E., Dewey R. J., Kramer M.,
McPhee C. A., 2006, MNRAS, 373, L50
- Weisberg J. M., Taylor J. H., 2002, ApJ, 576, 942
- Wex N., 2000, in Kramer M., Wex N., Wielebinski R., eds, Pulsar
Astronomy - 2000 and Beyond, IAU Colloquium 177. Astro-
nomical Society of the Pacific, San Francisco, p. 113
- Will C. M., 1993, Theory and Experiment in Gravitational
Physics. Cambridge University Press, Cambridge
- Will C. M., 2006, Living Reviews in Relativity, 9, 3